

Coronal lines and the importance of deep core-valence correlation in Ag-like ions

Jon Grumer,^{1,*} Ruifeng Zhao,^{2,3} Tomas Brage,¹ Wenxian Li,^{2,3} Sven Hultdt,⁴ Roger Hutton,^{2,3} and Yaming Zou^{2,3}

¹*Division of Mathematical Physics, Department of Physics, Lund University, Sweden*

²*The Key lab of Applied Ion Beam Physics, Ministry of Education, China*

³*Shanghai EBIT laboratory, Modern physics institute, Fudan University, Shanghai, China*

⁴*Lund Observatory, Lund University, Sweden*

(Dated: October 27, 2018)

We report on large-scale and critically evaluated *ab initio* MCDHF calculations of the wavelength of the "coronal", M1 transition $4f\ ^2F_{5/2}^o - ^2F_{7/2}^o$ in Ag-like ions. The transition between these two fine structure levels, which makes up the ground term for $Z \geq 62$ in the isoelectronic sequence, has recently been observed in Yb^{23+} and W^{27+} , where the latter could be of great importance for fusion plasma diagnostics. We present recommended values for all members of the sequence between $Z = 50$ and 94, which are supported by excellent agreement with values from recent experiments. The importance of including core-valence correlation with the $n = 3$ shell in the theoretical model is emphasized. The results show close to spectroscopic accuracy for these forbidden lines.

I. INTRODUCTION

Forbidden M1 transitions take place between states of the same parity. In particular such transitions among ground state levels in highly charged ions can be in the visible spectral region and have quite low transition rates. The most famous M1 transitions are the so-called *coronal lines* whose origin was unknown for more than 70 years before Edlén identified several of them as ground state M1 lines in 9-15 times ionized ions, mainly Ca, Fe and Ni in 1942 [1, 2]. Not for many years would it be possible to observe such lines in laboratory light sources. In 1978 Suckewer and Hinnov [3] made the first observation of an M1 transition in a fusion plasma. From the Doppler width of this line, 2665 Å in Fe XX, a record temperature (at that time) of 45×10^6 K was derived for the PLT tokamak. In Tokamaks, the solar corona, and in particular Electron Beam Ion Traps (EBITs) the plasma density is low enough for such lines to appear. In other terrestrial light sources for highly charged ions, e.g. sparks and laser produced plasmas, the long radiative lifetimes of the excited levels responsible for M1 transitions would lead to collisional quenching. It is interesting to note that Edlén could not observe the M1 lines he identified in the solar corona using contemporary laboratory light sources due to density problems. His identifications were based on his established energy levels from soft x ray spectroscopy. In the same way an attempt to establish the energy difference between the Ag-like ground state $4d^{10}4f\ ^2F_{5/2}^o$ and $^2F_{7/2}^o$ levels (for $Z \geq 62$), which is the subject of the work presented here, was only done through soft x ray spectroscopy [4].

The actual M1 transition connecting these two levels had not been observed before our work on Ag-like W [5] and recently Yb [6]. The lifetime of the upper level being in the millisecond range places interesting requirements

on the density of the light source. EBITs with electron densities on the order of 10^{12} cm^{-3} , or less, are ideal light sources for studying such transitions. Although the electron density in EBITs is lower than Tokamak fusion plasma densities, by around 2 orders of magnitude, M1 lines have been observed in fusion devices, e.g. as mentioned above the $2s^22p^3\ ^2D_{5/2} - ^2D_{3/2}$ M1 decay in Fe XX [3]. Also at the National Institute for Fusion Science in Japan Morita *et al.* [7] reported the observation of M1 transitions in the visible region for highly charged tungsten ions. Previously spectra from Tokamaks made a great impact on the study of M1 and other forbidden transitions (see [8] for details). With EBITs it is possible to measure both wavelengths and lifetimes of M1 [9] and even higher order transitions in highly charged ions, for example the studies of the M3 decay in Ni-like Xe [10] and later Ni-like W [11].

M1 transitions in highly charged ions with seemingly simple ground states such as the Ag-like $4d^{10}4f\ ^2F_{5/2,7/2}^o$ doublet are interesting testing grounds for theoretical methods since (a) for some ions along a sequence the M1 line will be a visible transition and therefore accessible to accurate measurement and (b) the calculation could be sensitive to correlation from deeper bound electrons, first noted in [5] and further investigated in this work. Finally (c) it is also possible that the results could be useful as a test of quantum-electrodynamical effects.

In the present work we use a systematic approach to calculate the wavelength of these M1 transitions in Ag-like ions. The $4d^{10}4f\ ^2F$ is the ground-term for ions with $Z > 61$, while at the neutral end the $4d^{10}5s\ ^2S$ forms the ground state. Adopting the Multiconfiguration Dirac-Hartree-Fock approach we carefully monitor the accuracy of the transition energy within different electron correlation models as a function of basis size. To further support the identification of these M1-lines, we use an isoelectronic analysis. The agreement between theory and experiment should be consistent for several ions and the trend of different atomic properties ought to behave smoothly as a function of the nuclear charge along the sequence.

*Electronic address: jon.grumer@teorfys.lu.se

Some previous isoelectronic work has been reported for theoretical work on Ag-like systems. Safronova *et al.* [12] used the Relativistic Many-Body Perturbation Theory (RMBPT) to study the energies of the singly excited states $4d^{10}\{4f, 5s, 5p, 5d, 5f, 5g\}$ for ions between $Z = 48$ and 100. The energy structures were unfortunately only tabulated for a few selected ions at the neutral end, but the rest was made available through the more recent publication of binding energies by Ivanova [13], from which it is possible to extract the $4f\ ^2F^o$ fine structure energy separations. Comparison with these results along the sequence provides a reliable benchmark for the present study, especially due to the different nature, perturbative versus variational, of the two methods. Ivanova also reported a few years earlier on calculations of Ag-like ions with $Z = 52$ to 86 based on Relativistic Perturbation Theory with a Model Potential (RPTMP) [14]. Finally there is a recent, but more limited in terms of correlation, MCDHF calculation by Ding *et al.* [15].

The aim of the present work is to use systematic isoelectronic analyses of electron correlation to provide solid support to the experimental identifications of the $4d^{10}4f\ ^2F_{5/2}^o - ^2F_{7/2}^o$ M1 transition in Ag-like W [5] and Yb [6] as well as future measurements in the mid- and, especially, high- Z range of the sequence. These new data should also, in addition to constituting a theoretical benchmark, be useful to the astrophysical- and fusion-plasma community.

II. METHOD OF CALCULATION

The $4f\ ^2F_{5/2,7/2}^o$ atomic wavefunctions are determined along the Ag I sequence using the Multiconfiguration Dirac-Hartree-Fock (MCDHF) method in the form of the most recently published version of the well-established fully relativistic GRASP2K code [16], originally developed by Grant and co-workers [17, 18].

A. Basic Multiconfiguration Dirac-Hartree-Fock theory

The MCDHF method is outlined in detail in Grant's book [19] and the non-relativistic variant of the approach is covered by Froese Fisher *et al.* [20]. Here we will only discuss the basic, and for our work most important, concepts.

The starting point for the MCDHF theory is to define an Atomic State Function (ASF), $|\Gamma J^\pi\rangle$, as a linear combination of Configuration State Functions (CSFs), $|\gamma_i J^\pi\rangle$;

$$|\Gamma J^\pi\rangle = \sum_i c_i |\gamma_i J^\pi\rangle, \quad (1)$$

where γ_i are labels to uniquely define the CSFs and c_i are expansion coefficients. The Γ is usually chosen as

the γ_i of the CSF with maximum weight c_i^2 . The CSFs are in turn anti-symmetrized products of single-electron Dirac orbitals coupled to Eigenfunctions of the total angular momentum (J^2 and J_z) and parity (π) operators. Without going into any details the MCDHF approach is essentially a multireference self-consistent field method based on the many-body Dirac-Coulomb Hamiltonian, expressed as

$$\mathcal{H}_{DC} = \sum_i^N h_D(\mathbf{r}_i) + \sum_{i>j}^N 1/r_{ij}, \quad (2)$$

in Hartree atomic units. Here h_D is the standard one-particle Dirac Hamiltonian and the second sum represents the instantaneous, inter-electronic Coulomb interaction.

The CSF basis expansion is generated in an Active Space (AS) approach in which a limited number of Dirac orbitals are divided into an inactive and active set. The CSF expansion is then formed through single (S), double (D), triple (T) etc. substitutions from a set of predefined important CSFs, the multireference (MR) set, to the active set of orbitals. A calculation on the MR set builds the zero order wavefunction. Orbitals of closed shells in the MR set are typically defined as inactive and therefore not a part of the active set.

The set of Dirac orbitals and mixing coefficients are optimized to self-consistency in the MCDHF procedure, followed by a relativistic configuration interaction (RCI) calculation in order to include the Breit interaction and leading QED effects. The Breit interaction is evaluated in the low frequency limit of the exchanged virtual photon. The contribution from vacuum polarization is included to second- (Uehling) and fourth-order (Källén-Sabry) [21]) and the self-energy is evaluated in the hydrogenic approximation with reference values from [22]).

The computational accuracy is essentially determined by whether the necessarily finite set of CSFs is effectively complete for the atomic states under investigation. This is dependent on the choice of included CSFs, but also on the optimization of and constraints on the Dirac orbitals. In practice the accuracy of the method is evaluated through careful convergence studies of atomic properties as a function of different correlation models and CSF-expansions within these models. The latter is defined by the size of the active set of correlation orbitals. In GRASP2K the calculations are performed in a layer-by-layer scheme, in which the AS of CSFs is enlarged systematically. The orbitals belonging to previous layers, defined by e.g. their principal quantum number n , are kept fixed in the variational procedure and only the new ones are optimized.

B. Correlation models

Two different computational models are presented in this work. The first (labeled SCV) is designed to provide

information about important correlation contributions. Based on the experience gained from this calculation it is possible to design a large-scale model (labeled FCV) with the goal of reaching high accuracy enough for what we could label as *single-line spectroscopy*.

Both models use $[1s^2 2s^2 \dots 4d^{10} 4f]_{5/2,7/2}^o$ as the MR set, i.e. two separate CSFs build the $J = 5/2$ and $7/2$ symmetry blocks. These CSFs are constructed from a common set of orbitals, optimized on a linear combination of the energies of the lowest state of each block (extended optimal level). In this work the Dirac-Fock method is defined as the case when the CSF expansion only includes the MR set. The orbitals obtained in the initial DF step are then kept frozen throughout the remaining procedure. To include correlation, the basis set is enlarged through substitutions from this reference configuration to a systematically increased set of CSFs.

A Separate Core-Valence (SCV) correlation model

In order to obtain an *ab initio* transition energy of close to spectroscopic accuracy, we need a detailed investigation of the correlation between valence and core electrons, or core-valence (CV) correlation. In the MCDHF scheme, CV correlation is represented by CSFs obtained from simultaneous replacements of one core and one valence electron of the CSFs in the MR set, with those in the active set of orbitals. In the special case of a singly occupied valence subshell, such as in the $4f$ configuration of Ag-like ions, the inclusion of CV correlation will in general increase the binding energy of this electron as compared to a fixed core calculation. The orbital of the single valence electron will therefore in many cases be contracted, which might have a large impact on different atomic properties.

CV correlation is often thought of as the MCDHF representation of core polarization. This is however a too simplistic interpretation. CV correlation does in general also include radial correlation through CSFs which only differ in the principal quantum number n from the reference CSFs. It is also clear that true core polarization should be evaluated by comparisons with results using core orbitals optimized on the bare core only, as the $4f$ -electron polarizes the core, and not with the DF results of the $|\dots 4d^{10} 4f \ ^2F^o\rangle$ states as we do here. We will therefore refer to core-valence correlation rather than core polarization.

Turning to the $4d^{10} 4f$ states of Ag-like ions, it was recently shown for Ag-like W [5] that a major part of the contribution from core-valence correlation to the fine structure separation $4f \ ^2F_{5/2,7/2}^o$ is due to interaction with the $3d$ subshell. This is maybe counter-intuitive as one would expect that the largest contributions should come from the outermost core subshells, i.e. $4d$ in this case. We will investigate this further along the Ag-like sequence.

Defining the singly occupied $4f$ subshell as the only va-

lence shell implies that there is no valence-valence (VV) correlation. This allows for separate studies of the energy contributions from interactions between the valence electron and the different core subshells, one subshell at a time. Such a Separate Core-Valence (SCV) study should provide valuable information about electron correlation, usable when designing a large-scale model including possible "interference" effects between contributions from different core subshells.

To be more specific, the SCV-calculations proceed with separate calculations for each subshell contribution, including only CSFs with one hole in a distinct core subshell. As an example, if we include only CSFs of the form $1s^2 2s^2 \dots 3p^5 \dots 4d^{10} nl n'l'$, where an electron from the $3p$ core subshell is allowed to be excited together with the $4f$ valence electron, we include CV correlation with $3p$. We aim in each calculation for converged results of the 2F energy separation, as a function of the maximum n and l of the orbitals included in the active set. Taking the difference of the converged and the DF energy separation gives an estimate of the energy contribution due to CV correlation with the chosen core subshell ($3p$ in our example). Adding all these SCV contributions to the DF energy value, gives an estimate of the total fine structure separation. It should be clear that this approach only is applicable to systems with a single valence electron since it otherwise is impossible to separate the VV and CV contributions.

Full Core-Valence (FCV) correlation model

With the results from the SCV model at hand, it is feasible to design a large-scale model in which CV correlation with all subshells (except $1s$) is included simultaneously in the MCDHF procedure. This will be referred to as the Full Core-Valence (FCV) model.

This model contains CSFs generated from simultaneous substitutions of at most one electron from any subshell down to $n = 2$, together with the $4f$ valence electron of the reference configuration to the active set of orbitals. The $1s$ subshell is kept closed as it proved having a negligible effect on the $^2F^o$ energy separation. Furthermore the CSFs of the $4d^8 4f^3$ configuration (the most important CSFs in the $n = 4$ complex in addition to $4d^{10} 4f$) are also added. The orbital set is increased up to $n = 10$ and $l = 6$ (i -orbitals), which corresponds to a maximum of 39 230 CFSs in the $J = 5/2$ block and 43 857 CSFs in the $J = 7/2$ block. These seem to be quite reasonably sized basis sets at first glance, but the calculation still takes a few weeks to run per charge state (with the serial version of the codes on modern 3.7 GHz Intel Xeon-based computers) due to comparatively dense energy matrices.

III. RESULTS AND DISCUSSION

We start this section with a discussion of the experiences gained from the smaller SCV model. This is followed by results from the large-scale FCV calculation, together with comparisons with other recent theoretical and experimental results. There is a special focus on the differences in the amount of core-valence correlation included in the different models and the impact of this on the final fine structure separations for different members of the isoelectronic sequence. In the final section we present rates for the magnetic-dipole transitions.

A. The impact of core-valence correlation

The SCV calculation reveals interesting trends of the effect of core-valence correlation on the fine structure separation along the isoelectronic sequence as can be seen in Fig. 1. In this plot the energy contribution due to CV correlation with all core subshells down to $2s$ is presented for ions between $Z = 50$ and 92 . For the ions at the neutral end it is clear that the CV contribution from $4d$ is large as would be expected. However, for $Z \geq 58$ the major contribution is due to $3d$ and it becomes increasingly dominant as Z increases, followed by CV correlation with $3p$ and $4p$. For $Z = 94$ the correlation with $3d$ makes up 46% of the total contribution. It is also interesting to note that the impact of correlation with $4d$ becomes almost negligible for $Z \geq 70$ and actually gives a negative contribution for $70 < Z < 85$. The fact that CV correlation with deeper core shells becomes an important factor in the calculation of this fine structure separation was first noted for Ag-like W ($Z = 74$) [5] where correlation with $3d$ contributes with 51% of the total value and the whole $n = 3$ shell 78%.

Judging from the results of this initial investigation, one can conclude that core-valence correlation with essentially all core subshells is of importance to the fine structure separation when aiming for high accuracy. In the low- Z regime it's clear that interactions with the $n = 4$ subshells are crucial, replaced by $3p$ and foremost $3d$ for higher members of the sequence.

B. The $4f$ ${}^2F^o$ fine structure separation from the FCV model

In this section we present results from ${}^2F^o$ energy separations along the Ag-like isoelectronic sequence from the large-scale FCV model in which core-valence correlation is included with all subshells except $1s$. The model has been carefully evaluated in terms of convergence of the energy separation of ${}^2F^o$ with respect to the size of the active set of Dirac orbitals. Within the boundaries of this model it can be seen from Fig. 2, which shows the convergence trend (difference in energy from previous correlation layer as a fraction of the total fine structure) in a

logarithmic scale, that the fine structure separation has been converged to close to 0.1% for $Z = 56$ and to 0.006% for $Z = 90$.

Resulting energies for all ions in the Ag-like isoelectronic sequence with nuclear charges $50 \leq Z \leq 94$ are presented in Tab. I and Fig. 3. In the second column we give the Dirac-Fock energies from the MCDHF (Dirac-Coulomb) approach, where a negative value corresponds to an inverted fine structure. The third column contains energy contributions due to the frequency independent Breit interaction, and the fourth shows leading QED effects. The impact of electron correlation in the regime of the Dirac-Coulomb-Breit-QED Hamiltonian (calculated by taking the difference of the DF and the converged FCV results) is presented in the fifth column. Finally the sixth column and Fig. 3 give the total energy separation including all the above mentioned contributions. It is clear that correlation is the dominating correction to DF (Dirac-Coulomb) in the low- Z regime, replaced by the Breit interaction for $Z \geq 57$. The energy shift due to the QED corrections are comparatively small along the whole sequence.

C. Comparison with experiment and other theory

The fine structure energy separations from experimental and other theoretical results are compared to our FCV values in Tab. II and plotted as differences to our FCV results in Fig. 4. As shown in Fig. 3, the trend of the fine structure splitting along the sequence should be smooth, in the absence of level crossing or other effects. We should therefore expect a similar behavior for other methods and thereby also for the difference between different sets of results.

The agreement of our results with most of the experimental data points is in general very good, with the largest deviations between $Z = 62$ to 66 , where the $4d^{10}4f$ ${}^2F^o$ term becomes ground state ($Z = 62$). The experimental values do show, however, an irregular isoelectronic trend for low- Z ions, which do warrant further investigations. For higher nuclear charges there are excellent agreement (less than 0.1%) with the two most recent experimental results: 19383 cm^{-1} for Yb ($Z = 70$) [6] and 29600 cm^{-1} for W ($Z = 74$) [5].

There is also a good agreement between our results and the relativistic many-body perturbation theory (RMBPT) calculation, especially in the beginning and high-end of the sequence. More importantly in the two ends, the difference between the two data sets behaves in smooth way, except for the leap between $Z = 57$ and 61 . It is important to note, however, that the RMBPT values are collected from two sets of data, presented in two different publications ($Z \leq 57$ from Safronova *et al.* [12] and $Z \geq 61$ from Ivanova [13]). The leap in energy might therefore be due to some inconsistency between the two papers or in the model. Another possibility is close degeneracy caused by level crossings as the $4f$ configura-

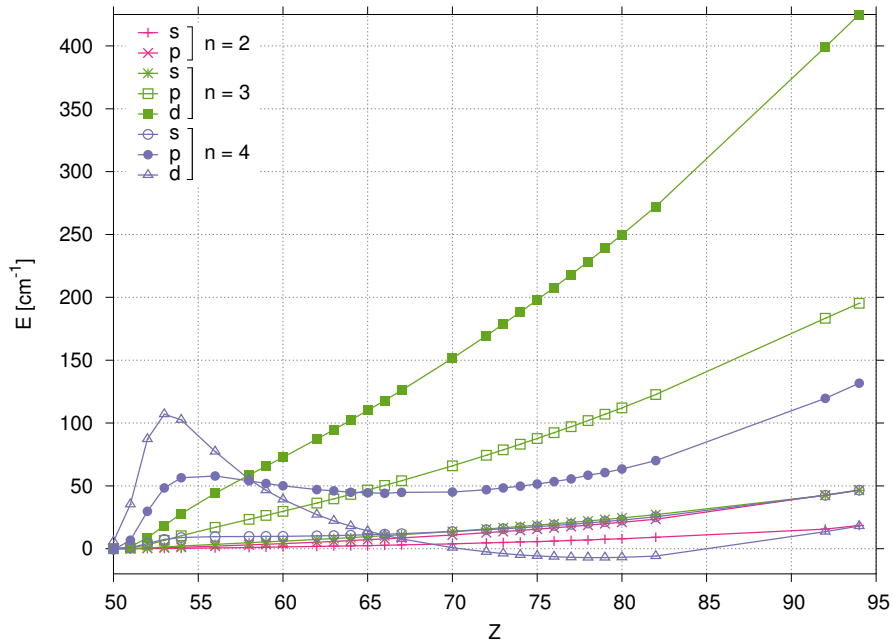


FIG. 1: Absolute contributions from core-valence correlation with different core subshells relative to Dirac-Fock energies ($E = E_{\text{tot}}^{\text{SCV}}(nl) - E_{\text{DF}}$, the SCV model is explained in the text) to the $4f^2F^o$ fine structure energy separation of Ag-like ions with nuclear charges $50 \leq Z \leq 94$. This clearly shows the dominating behavior of core-valence correlation with $3d$ rather than $4d$ in the mid- and high- Z regime. Note that these energy contributions are presented as absolute numbers and not as a fraction of the total fine structure energy separation, to compared with Tab. I or Fig. 3 where the total energies are given.

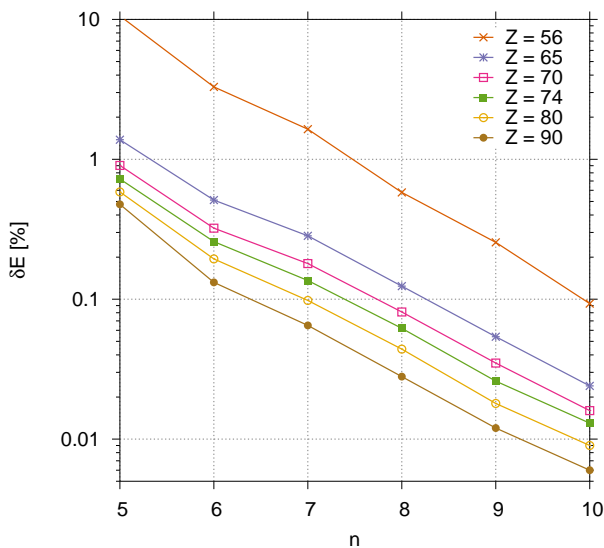


FIG. 2: Relative convergence of the $2F^o$ energy separation as the size of the active set of orbitals is increased in a layer-by-layer scheme, denoted by the principal quantum number n . δE is the difference in percentages of energy from the previous correlation layer.

tion becomes the ground state, which could be difficult to represent in a perturbative approach.

The difference between our results and the earlier MCDHF calculation [15] is most likely explained by their

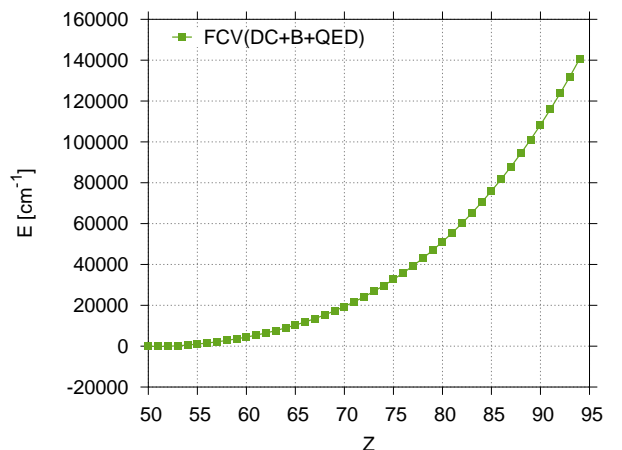


FIG. 3: Energies of the $4d^{10} 4f^2F^o$ fine structure separation from our FCV calculation along the Ag-like isoelectronic sequence.

exclusion of core-valence correlation with other subshells than $4d$. From the earlier discussion about the SCV investigation, presented in Fig. 1, it was made clear the $n = 3$ shell contributes around 78% of the total amount of core-valence correlation whereas the $4d$ subshell barely contributes at all for this Z . It is however hard to understand the irregular isoelectronic behavior of their results.

Finally it is clear that there is a large inconsistency between the RPTMP results [14] and all other methods pre-

TABLE I: The fine structure separation of $4f\ ^2F_{5/2,7/2}^o$ from the Full Core-Valence (FCV) calculation (see text for details). The first column shows the atomic number, Z and the second ($E_{\text{DF}}^{\text{DC}}$) gives the energy separations resulting from single-CSF calculations, here referred to as Dirac-Fock (DF), based on the Dirac-Coulomb (DC) Hamiltonian. The third column (δE_{B}) presents additional energy contributions due to the Breit interaction in the low-frequency limit (B). The fourth (δE_{QED}) presents the total contribution from self-energy and vacuum polarization (QED) corrections. The fifth column (δE_{corr}) shows how big the influence of correlation is in the DC+B+QED scheme. In the sixth column (E_{tot}) the total energy separations (including Breit, QED and correlation) are presented. All energies are given in cm^{-1} and a negative total energy value corresponds to an inverted fine structure (i.e. the $J = 7/2$ level having lowest energy).

Z	$E_{\text{DF}}^{\text{DC}}$	$+\delta E_{\text{B}}$	$+\delta E_{\text{QED}}$	$+\delta E_{\text{corr}}$	$= E_{\text{tot}}$	Z	$E_{\text{DF}}^{\text{DC}}$	$+\delta E_{\text{B}}$	$+\delta E_{\text{QED}}$	$+\delta E_{\text{corr}}$	$= E_{\text{tot}}$
50	-88	-3	0	6	-85	73	27826	-1400	20	341	26786
51	-182	-13	0	59	-136	74	30750	-1510	22	358	29619
52	-161	-37	0	157	-41	75	33876	-1626	25	376	32651
53	62	-70	0	213	205	76	37215	-1747	27	394	35890
54	441	-106	0	229	564	77	40774	-1873	31	414	39346
55	925	-145	1	229	1010	78	44564	-2005	34	436	43028
56	1495	-186	1	225	1535	79	48592	-2143	37	458	46945
57	2145	-229	1	221	2139	80	52869	-2286	41	481	51106
58	2877	-274	2	218	2823	81	57405	-2435	45	506	55521
59	3696	-323	2	217	3592	82	62209	-2590	50	531	60199
60	4606	-374	3	217	4451	83	67290	-2752	55	557	65151
61	5613	-429	3	219	5406	84	72660	-2919	60	585	70385
62	6724	-488	4	223	6463	85	78329	-3093	65	613	75914
63	7946	-550	5	227	7628	86	84307	-3274	71	643	81747
64	9286	-616	5	234	8909	87	90604	-3461	77	674	87894
65	10749	-686	6	241	10311	88	97232	-3656	84	706	94366
66	12344	-760	8	250	11842	89	104201	-3857	91	740	101175
67	14078	-838	9	260	13509	90	111524	-4065	98	774	108331
68	15958	-920	10	271	15320	91	119210	-4280	106	810	115845
69	17992	-1006	12	283	17280	92	127272	-4503	114	847	123729
70	20188	-1098	13	295	19399	93	135721	-4734	122	886	131995
71	22554	-1193	15	310	21685	94	144569	-4972	132	925	140654
72	25097	-1294	17	325	24145						

sented here, since the isoelectronic trend deviates from those predicted by others and shows inexplicable leaps.

To analyze the different theoretical methods and experiments further, we plot the contribution to the fine structure separation due to electron correlation in Fig. 5. This is defined as the best available value (theoretical or experimental) from which the Dirac-Fock value is subtracted. This again reveals a good agreement between our results and experiment, in terms of the individual data points and in the isoelectronic trend. The RMBPT results also agree well with both our results and the experimental values. Comparing this plot with Fig. 4 one can conclude that the earlier MCDHF [15] calculation lacks a major bulk of electron correlation necessary to reach a fine structure separation close to experimental results. The irregular trend along the sequence mentioned above, especially the dip in energy around $Z = 65$, remains unexplained.

D. Magnetic-dipole transition probabilities

The calculation of the magnetic-dipole (M1) transition rate is almost trivial once the correct transition energy has been found, since the M1 operator is independent of the radial part of the wavefunction. In Tab. III the (vacuum) wavelength of the transition is presented along the isoelectronic sequence, together with the corresponding rates, weighted oscillator strengths and line strengths. The simplicity of the M1 transition rate is reflected in the almost constant behavior of the line strength (which is independent of the transition energy). The small decrease seen with increasing Z is due to the CSF composition of the wavefunctions of the involved states, via interaction with other LS -terms than $^2F^o$. This effect is however small since the ground term $^2F^o$ is well-isolated in energy for most of the ions in the sequence.

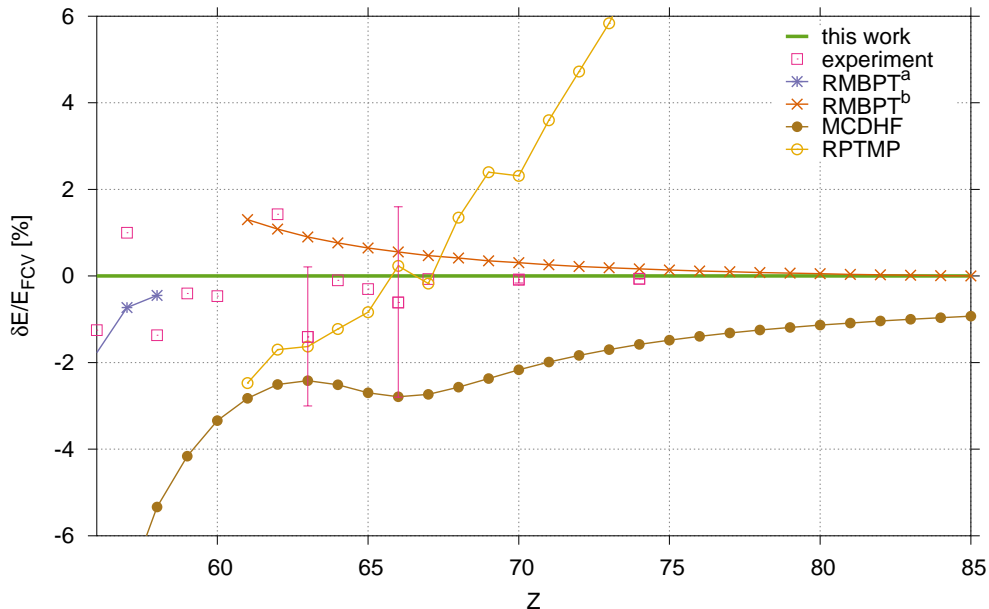


FIG. 4: Experimental (see Tab. II for sources) and other theoretical (RMBPT^a [12], RMBPT^b [12] (from [13]), MCDHF [15] and RPTMP [13, 14]) energies presented for an interesting sub-range ($56 \geq Z \geq 85$) of the Ag-like isoelectronic sequence. The energy separations of the different sources are plotted as fractional differences relative to the FCV calculation $\delta E/E_{\text{FCV}}^{\text{tot}} = (E_{\text{method}} - E_{\text{FCV}}^{\text{tot}})/E_{\text{FCV}}^{\text{tot}}$ in percentages. Error bars of four experimental data points were available and are included in the plot.

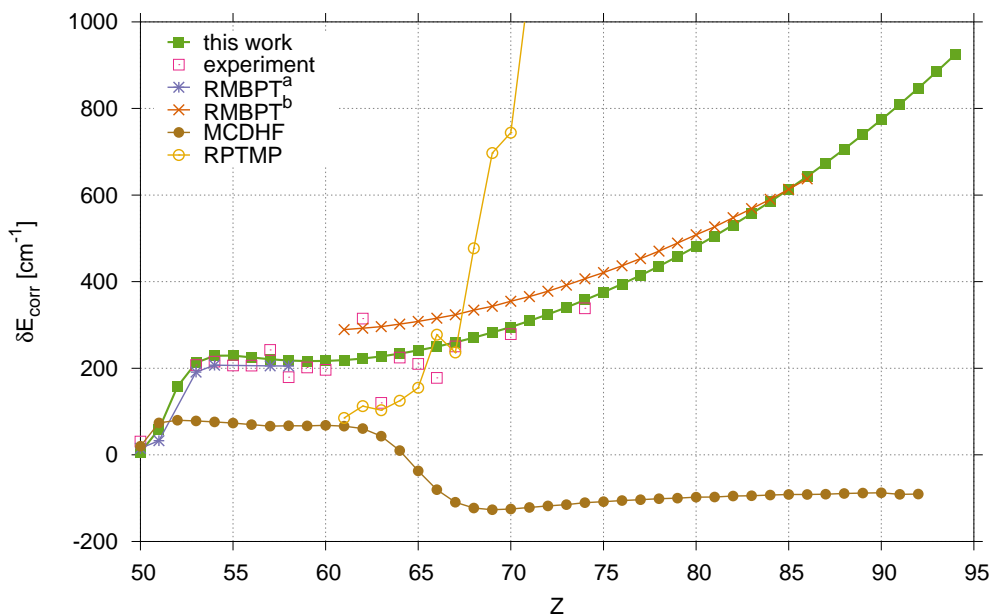


FIG. 5: Estimated absolute contributions from core-valence correlation to the $4f \ ^2F^o$ fine structure separation ($\delta E_{\text{corr}} = E_{\text{method}} - E_{\text{DF}}^{\text{FCV}}$ where the "method" superscript should be replaced by the corresponding label in the legend) for experiment and other available theory (RMBPT^a [12], RMBPT^b [12] (from [13]), MCDHF [15] and RPTMP [13, 14]).

IV. CONCLUSIONS

In this work we have presented a systematic MCDHF study of the $4f \ ^2F^o$ fine structure separation and the involved magnetic-dipole transition for Ag-like ions with nuclear charges $Z = 50 - 94$. Special attention has been

paid to core-valence effects with deep core subshells and it was shown that core-valence correlation with $3d$, rather than $4d$, is the dominant contributor for intermediate and highly charged ions. The underlying reason for this could be an interesting case for further studies. Our large-scale MCDHF calculations include correlation ef-

TABLE II: Comparison of the $4f\ ^2F_{5/2,7/2}^c$ energy separation obtained from the large-scale FCV model ($E_{\text{tot}}^{\text{FCV}}$) with experiment (E_{exp}) (corresponding source(s) are given in the fourth column), and other available theory (E_{RMBPT} [12], E_{MCDHF} [15] and E_{RPTMP} [13, 14]). All energies are given in cm^{-1} and the differences are presented relative to the FCV values of this work in absolute numbers δ_E and in percentages $\delta\%$.

Z	$E_{\text{tot}}^{\text{FCV}}$	E_{exp}	Source	δ_E	$\delta\%$	E_{RMBPT}	δ_E	$\delta\%$	E_{MCDHF}	δ_E	$\delta\%$	E_{RPTMP}	δ_E	$\delta\%$
50	-85	-60	[23, 24]	-24	40%	-76	-9	12%	-71	-14	20%			
51	-136					-162 ^b	26	-16%	-121	-15	12%			
52	-41								-118	77	-66%			
53	205	200	[25]	5	2.7%	184	21	12%	71	134	189%			
54	564	550	[24, 26]	14	2.5%	542	22	4.0%	411	153	37%			
55	1010	987	[24, 27]	23	2.3%				854	156	18%			
56	1535	1516	[24, 28]	19	1.3%				1380	155	11%			
57	2139	2160	[25]	-21	-1.0%	2123	16	0.7%	1984	155	7.8%			
58	2823	2784	[29]	39	1.4 %	2810	13	0.4%	2672	151	5.6%			
59	3592	3577	[29]	15	0.4 %				3442	150	4.3%			
60	4451	4430	[29]	21	0.5 %				4302	149	3.5%			
61	5406					5476 ^c	-70	-1.3%	5253	153	2.9%	5272	134	2.5%
62	6463	6555	[29]	-92	-1.4%	6533 ^c	-70	-1.1%	6301	162	2.6%	6353	110	1.7%
63	7628	7521 \pm 62	[29]	107	1.4%	7697 ^c	-69	-0.9%	7444	184	2.5%	7504	124	1.7%
64	8909	8900	[29] ^a	9		8977 ^c	-68	-0.8%	8685	224	2.6%	8800	109	1.2%
65	10311	10280	[29]	31	0.3%	10378 ^c	-67	-0.6%	10033	278	2.8%	10225	86	0.8%
66	11842	11770 \pm 131	[29]	72	0.6%	11908 ^c	-66	-0.6%	11512	330	2.9%	11870	-28	0.2%
67	13509	13500	[29] ^a	9	0.1%	13573 ^c	-64	-0.5%	13140	369	2.8%	13486	23	0.2%
68	15320					15383 ^c	-63	-0.4%	14926	394	2.6%	15526	-206	-1.3%
69	17280					17341 ^c	-61	-0.3%	16871	409	2.4%	17695	-415	-2.3%
70	19399	19383 \pm 8	[6]	16	0.1%	19459 ^c	-60	-0.3%	18979	420	2.2%	19848	-449	-2.3%
71	21685					21741 ^c	-56	-0.3%	21254	431	2.0%	22465	-780	-3.5%
72	24145					24198 ^c	-53	-0.2%	23702	443	1.9%	25285	-1140	-4.5%
73	26786					26838 ^c	-52	-0.2%	26331	455	1.7%	28350	-1564	-5.5%
74	29619	29600 \pm 2	[5]	19	0.1%	29668 ^c	-49	-0.2%	29151	468	1.6%	31769	-2150	-6.8%
75	32651					32696 ^c	-45	-0.1%	32167	484	1.5%	35494	-2843	-8.0%
76	35890					35932 ^c	-42	-0.1%	35390	500	1.4%	39491	-3601	-9.1%
77	39346					39385 ^c	-39	-0.1%	38828	518	1.3%	43765	-4419	-10%
78	43028					43063 ^c	-35	-0.1%	42491	537	1.3%	48320	-5292	-11%
79	46945					46976 ^c	-31	-0.1%	46387	558	1.2%	53411	-6466	-12%
80	51106					51133 ^c	-27	-0.1%	50527	579	1.1%	58754	-7648	-13%
81	55521					55542 ^c	-21	0.0 %	54918	603	1.1%	64649	-9128	-14%
82	60199					60216 ^c	-17	0.0 %	59573	626	1.1%	70791	-10592	-15%
83	65151					65162 ^c	-11	0.0 %	64499	652	1.0%	77338	-12187	-16%
84	70385					70391 ^c	-6	0.0 %	69708	677	1.0%	84066	-13681	-16%
85	75914					75914 ^c	0	0.0 %	75209	705	0.9%	91483	-15569	-17%
86	81747					81741 ^c	6	0.0 %	81012	735	0.9%	99145	-17398	-18%
87	87894								87129	765	0.9%			
88	94366								93571	795	0.8%			
89	101175								100347	828	0.8%			
90	108331								107469	862	0.8%			
91	115845								114944	901	0.8%			
92	123729								122792	937	0.8%			
93	131995													
94	140654													

^a based on interpolated values of $4f\ ^2F_{7/2}^c$ [29]

^b from Tab. 8 in Ref. [14]

^c from Tab. 11 in Ref. [13]

TABLE III: Wavelengths in vacuum (λ_{vac}), transition rates (A), weighted oscillator strengths (gf) and line strengths (S) of the $4f\ ^2F_{5/2}^o - ^2F_{7/2}^o$ magnetic-dipole (M1) transition of Ag-like ions between $Z = 50$ and 94 from the large-scale FCV calculation. Note that the $J = 7/2$ is the lowest level up to and including $Z = 52$, then the two levels cross and $J = 5/2$ becomes the lower of the two from $Z \geq 53$. Numbers in square brackets denotes powers of ten.

Z	λ_{vac} (Å)	A (s^{-1})	gf	S	Z	λ_{vac} (Å)	A (s^{-1})	gf	S
50	1.176[+6]	9.463[-6]	1.178[-8]	3.428	73	3.733[+3]	2.216[+2]	3.703[-6]	3.419
51	7.378[+5]	3.837[-5]	1.879[-8]	3.428	74	3.376[+3]	2.995[+2]	4.094[-6]	3.418
52	2.459[+6]	1.036[-6]	5.638[-9]	3.428	75	3.063[+3]	4.011[+2]	4.513[-6]	3.418
53	4.870[+5]	1.000[-4]	2.846[-8]	3.428	76	2.786[+3]	5.326[+2]	4.960[-6]	3.417
54	1.774[+5]	2.070[-3]	7.814[-8]	3.428	77	2.542[+3]	7.017[+2]	5.436[-6]	3.417
55	9.902[+4]	1.190[-2]	1.400[-7]	3.427	78	2.324[+3]	9.175[+2]	5.944[-6]	3.416
56	6.514[+4]	4.180[-2]	2.127[-7]	3.427	79	2.130[+3]	1.191[+3]	6.484[-6]	3.415
57	4.676[+4]	1.130[-1]	2.963[-7]	3.426	80	1.957[+3]	1.537[+3]	7.057[-6]	3.415
58	3.543[+4]	2.598[-1]	3.910[-7]	3.426	81	1.801[+3]	1.970[+3]	7.666[-6]	3.414
59	2.784[+4]	5.350[-1]	4.975[-7]	3.425	82	1.661[+3]	2.511[+3]	8.310[-6]	3.414
60	2.247[+4]	1.018[+0]	6.164[-7]	3.425	83	1.535[+3]	3.182[+3]	8.992[-6]	3.413
61	1.850[+4]	1.824[+0]	7.486[-7]	3.425	84	1.421[+3]	4.012[+3]	9.712[-6]	3.412
62	1.547[+4]	3.117[+0]	8.949[-7]	3.424	85	1.317[+3]	5.032[+3]	1.047[-5]	3.412
63	1.311[+4]	5.124[+0]	1.056[-6]	3.424	86	1.223[+3]	6.283[+3]	1.128[-5]	3.411
64	1.123[+4]	8.161[+0]	1.233[-6]	3.423	87	1.138[+3]	7.807[+3]	1.212[-5]	3.410
65	9.698[+3]	1.265[+1]	1.427[-6]	3.423	88	1.060[+3]	9.660[+3]	1.301[-5]	3.410
66	8.444[+3]	1.916[+1]	1.639[-6]	3.422	89	9.884[+2]	1.190[+4]	1.395[-5]	3.409
67	7.402[+3]	2.845[+1]	1.869[-6]	3.422	90	9.231[+2]	1.461[+4]	1.493[-5]	3.408
68	6.528[+3]	4.148[+1]	2.120[-6]	3.421	91	8.632[+2]	1.786[+4]	1.596[-5]	3.407
69	5.787[+3]	5.952[+1]	2.391[-6]	3.421	92	8.082[+2]	2.176[+4]	1.705[-5]	3.407
70	5.155[+3]	8.420[+1]	2.683[-6]	3.420	93	7.576[+2]	2.641[+4]	1.818[-5]	3.406
71	4.612[+3]	1.176[+2]	2.999[-6]	3.420	94	7.110[+2]	3.195[+4]	1.937[-5]	3.405
72	4.142[+3]	1.623[+2]	3.339[-6]	3.419					

fects from Coulomb- and (frequency independent) Breit interaction, as well as corrections due to dominant QED effects. The accuracy of the $^2F^o$ fine structure separation is carefully analyzed through systematic studies of convergence trends as the active set of virtual Dirac-orbitals, used to construct the many-body basis, is increased. This is augmented by studies of the smoothness of different properties along the isoelectronic sequence. Furthermore, a good agreement with experiments, of which some are very recent EBIT measurements [5, 6], and other reliable theoretical results, finally leads us to conclude that our method provides accurate data for the $^2F^o$ levels of Ag-like ions. Transition rates, weighted oscillator strengths and line strengths of the magnetic-dipole transition between these two fine structure levels have been calculated and tabulated. These data should be accurate since the M1 operator is not dependent on the radial part of

the wavefunctions, and the transitions energies are accurately predicted.

V. ACKNOWLEDGMENTS

This work was supported by the National Natural Science Foundation of China under project no. 11074049, and by the Shanghai Leading Academic Discipline Project B107. We also gratefully acknowledge support from the Swedish Research Council (Vetenskapsrådet) and the Swedish Institute under the Visby-programme. JG and WL would like to especially thank the Nordic Centre at Fudan University for supporting an exchange between Lund and Fudan. Finally the authors would like to thank Gordon Berry, Jörgen Ekman and Per Jönsson for valuable discussions.

[1] B. Edlén, Zeitschrift für Astrophysik **22**, 30 (1943).

[2] B. Edlén, Monthly Notices of the Royal Astronomical Society **105**, 323 (1945).

[3] S. Suckewer and E. Hinnov, Phys.

Rev. Lett. **41**, 756 (1978), URL <http://link.aps.org/doi/10.1103/PhysRevLett.41.756>.

[4] J. Sugar and V. Kaufman, Phys. Rev. A **21**, 2096 (1980), URL

- <http://link.aps.org/doi/10.1103/PhysRevA.21.2096>.
- [5] Z. Fei, R. Zhao, Z. Shi, J. Xiao, M. Qiu, J. Grumer, M. Andersson, T. Brage, R. Hutton, and Y. Zou, *Physical Review A* **86**, 062501 (2012).
- [6] R. Zhao, private communication (2014).
- [7] S. Morita, C. F. Dong, M. Goto, D. Kato, I. Murakami, H. A. Sakaue, M. Hasuo, F. Koike, N. Nakamura, T. Oishi, et al., *AIP Conference Proceedings* **1545**, 143 (2013), URL <http://scitation.aip.org/content/aip/proceeding/aipcp/1003/1545/143>.
- [8] I. Martinson and C. Jupén, *Journal of the Chinese Chemical Society* **48**, 469 (2001), ISSN 2192-6549, URL <http://dx.doi.org/10.1002/jccs.200100070>.
- [9] A. Lapierre, U. Jentschura, J. C. López-Urrutia, J. Braun, G. Brenner, H. Bruhns, D. Fischer, A. G. Martínez, Z. Harman, W. Johnson, et al., *Phys. Rev. Lett.* **95**, 183001 (2005), URL <http://link.aps.org/doi/10.1103/PhysRevLett.95.183001>.
- [10] E. Träbert, P. Beiersdorfer, and G. V. Brown, *Phys. Rev. Lett.* **98**, 263001 (2007), URL <http://link.aps.org/doi/10.1103/PhysRevLett.98.263001>.
- [11] Y. Ralchenko, *Journal of Physics B: Atomic, Molecular and Optical Physics* **40**, F175 (2007), URL <http://stacks.iop.org/0953-4075/40/i=11/a=F01>.
- [12] U. I. Safronova, I. M. Savukov, M. S. Safronova, and W. R. Johnson, *Phys. Rev. A* **68**, 062505 (2003), URL <http://link.aps.org/doi/10.1103/PhysRevA.68.062505>.
- [13] E. Ivanova, *Atomic Data and Nuclear Data Tables* **97**, 1 (2011).
- [14] E. Ivanova, *Atomic Data and Nuclear Data Tables* **95** (2009).
- [15] X.-B. Ding, F. Koike, I. Murakami, D. Kato, H. A. Sakaue, C.-Z. Dong, and N. Nakamura, *Journal of Physics B: Atomic, Molecular and Optical Physics* **45**, 035003 (2012).
- [16] P. Jönsson, G. Gaigalas, J. Bieroń, C. F. Fischer, and I. P. Grant, *Computer Physics Communications* **184**, 2197 (2013), ISSN 0010-4655, URL <http://www.sciencedirect.com/science/article/pii/S0010465513003407>.
- [17] K. Dyall, I. Grant, C. Johnson, F. Parpia, and E. Plummer, *Computer Physics Communications* **55**, 425 (1989).
- [18] F. A. Parpia, C. F. Fischer, and I. P. Grant, *Computer physics communications* **94**, 249 (1996).
- [19] I. P. Grant, *Relativistic Quantum Theory of Atoms and Molecules: Theory and Computation (Springer Series on Atomic, Optical, and Plasma Physics)* (Springer-Verlag New York, Inc., Secaucus, NJ, USA, 2006), ISBN 03874015848.
- [20] C. Froese Fischer, T. Brage, and P. Jönsson, *Computational atomic structure: an MCHF approach* (Inst. of Physics Publishing, Bristol, 1997).
- [21] L. W. Fullerton and G. A. Rinker, *Phys. Rev. A* **13**, 1283 (1976), URL <http://link.aps.org/doi/10.1103/PhysRevA.13.1283>.
- [22] P. J. Mohr, *Atomic Data and Nuclear Data Tables* **29**, 453 (1983), ISSN 0092-640X, URL <http://www.sciencedirect.com/science/article/pii/S0092640X8300026>.
- [23] C. Moore, *Stand. Ref. Data Ser., Nat. Bur. Stand.(US)* **35** (1971).
- [24] A. Kramida, Y. Ralchenko, J. Reader, and NIST ASD Team, *NIST Atomic Spectra Database (ver. 5.0)* [Online] p. <http://www.nist.gov/pml/data/asd.cfm> (2012), URL [Online]<http://physics.nist.gov/asd>.
- [25] V. Kaufman and J. Sugar, *Physica Scripta* **24**, 738 (1981).
- [26] M. O. Larsson, A. M. Gonzalez, R. Hallin, F. Heijkensköld, R. Hutton, A. Langereis, B. Nyström, G. O'Sullivan, and A. Wännström, *Physica Scripta* **51**, 69 (1995), URL <http://stacks.iop.org/1402-4896/51/i=1/a=011>.
- [27] A. Tauheed and Y. Joshi, *Physica Scripta* **72**, 385 (2005).
- [28] S. Churilov and Y. Joshi, *Physica Scripta* **62**, 282 (2000).
- [29] J. Sugar and V. Kaufman, *Physica Scripta* **24**, 742 (1981).